

Polar twin boundaries and nonconventional ferroelectric switching

Ekhard K. H. Salje, Suzhi Li, Ziyuan Zhao, Peter Gumbsch, and Xiangdong Ding

Citation: [Applied Physics Letters](#) **106**, 212907 (2015); doi: 10.1063/1.4922036

View online: <http://dx.doi.org/10.1063/1.4922036>

View Table of Contents: <http://scitation.aip.org/content/aip/journal/apl/106/21?ver=pdfcov>

Published by the [AIP Publishing](#)

Articles you may be interested in

[Enhancement of fatigue endurance in ferroelectric PZT ceramic by the addition of bismuth layered SBT](#)

J. Appl. Phys. **116**, 164105 (2014); 10.1063/1.4899237

[Highly mobile vortex structures inside polar twin boundaries in SrTiO₃](#)

Appl. Phys. Lett. **104**, 082907 (2014); 10.1063/1.4866859

[Domain evolution in ferroelectric thin films during fatigue process](#)

J. Appl. Phys. **97**, 104102 (2005); 10.1063/1.1894603

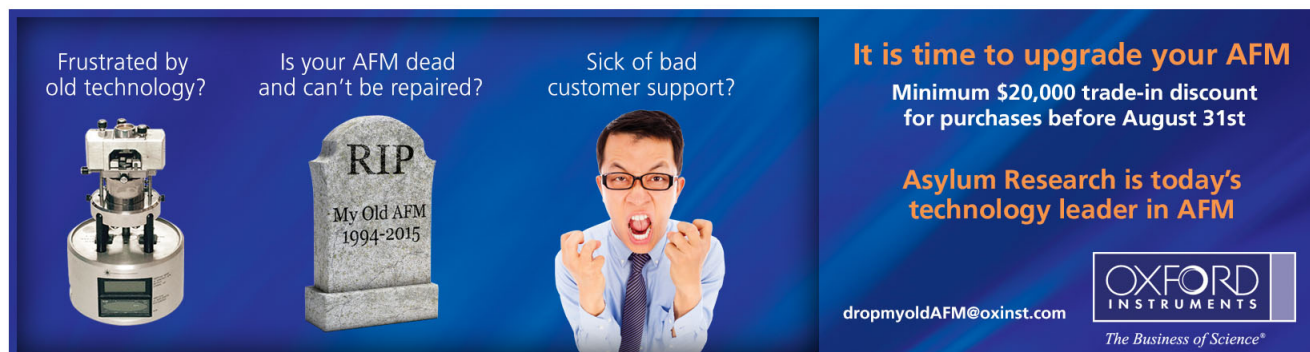
[Ferroelectric hysteresis loops of \(Pb, Ca\)TiO₃ thin films under spherical indentation](#)

Appl. Phys. Lett. **85**, 2023 (2004); 10.1063/1.1787594


[Fatigue study of metalorganic-decomposition-derived SrBi₂Ta₂O₉ thin films: The effect of partial switching](#)

Appl. Phys. Lett. **76**, 2208 (2000); 10.1063/1.126298


Frustrated by old technology?



Is your AFM dead and can't be repaired?



Sick of bad customer support?




It is time to upgrade your AFM

Minimum \$20,000 trade-in discount for purchases before August 31st

Asylum Research is today's technology leader in AFM

dropmyoldAFM@oxinst.com



The Business of Science®

Polar twin boundaries and nonconventional ferroelectric switching

Ekhard K. H. Salje,^{1,a)} Suzhi Li,² Ziyuan Zhao,^{1,3} Peter Gumbsch,^{2,4} and Xiangdong Ding³

¹Department of Earth Sciences, University of Cambridge, Cambridge CB2 3EQ, United Kingdom

²Institute for Applied Materials, Karlsruhe Institute of Technology, Karlsruhe 76131, Germany

³State Key Laboratory for Mechanical Behavior of Materials, Xi'an Jiaotong University, Xi'an 710049, China

⁴Fraunhofer Institute for Mechanics of Materials IWM, Freiburg 79108, Germany

(Received 14 April 2015; accepted 21 May 2015; published online 29 May 2015)

Polar twin wall properties in non-polar or weakly polar matrices can be switched by electric fields with a well-defined ferroelectric hysteresis. While the bulk is nonpolar or weakly polar, the ferroelectric hysteresis stems from the interplay of the field-induced polarization in the bulk and the rotation of the dipole moments in the twin walls. While each tilt of a dipole would be a linear function of the applied field, their combination leads to frustration: The boundary polarity hinders the development of the bulk polarity for weak fields perpendicular to the twin walls. Only when the boundary polarity is sufficiently rotated under stronger fields do we find a sudden collapse of the frustration and the rapid development of bulk polarity. This effect suggests that wall polarity (as observed in CaTiO_3 and SrTiO_3) may lead to nonconventional ferroelectric switching including the bulk rather than exclusively inside domain walls. © 2015 AIP Publishing LLC.

[<http://dx.doi.org/10.1063/1.4922036>]

The quest for advanced nano-scale ferroic materials has lead to two major developments. The first approach focuses on interfaces between two different materials (e.g., organic inorganic interfaces,¹ two different perovskite structures,^{2,3} or interfaces between segments of the same material with different crystallographic orientations (bi-crystals).⁴ The second approach starts from ferroelastic twin boundaries, where functionalities are generated by subtle structural changes inside the twin boundary. Such twin boundaries were already found to be superconducting,⁵ ferroelectric,^{6–9} or magnetic,¹⁰ while the same properties do not exist in the bulk. This path is commonly known as domain boundary engineering^{11,12} and has the main advantage that the template structures may contain complex patterns of many ferroelastic twin boundaries,¹³ which can be tailored by external forces. In case of ferroelectric memory devices, the memory density can then be massively increased because the functional parts of a device material are not the bulk but twin boundaries or anti-phase boundaries, APBs, which can be produced in different densities and geometrical pattern.^{14–22}

This idea was advanced further²³ by showing that planar twin boundaries contain yet a finer scale nano-structure that was previously ignored, namely, polar one-dimensional Bloch lines^{24,25} and vortex points between such Bloch lines. Bloch lines contain polar dipoles perpendicular to the twin wall. These dipoles can be switched by an electric field so that Bloch line can be ferroelectric. It was argued that Bloch line switching requires only weak electric fields and therefore can serve as memory elements. The density of these Bloch lines is expected to be higher than the density of twin walls.

If the bulk is either nonpolar or weakly polar, one may ask what happens if the much stronger wall-dipoles interact with weaker dipoles in the bulk? We show in this paper that wall polarity remains stable and that it generates “vortex structures” amongst bulk dipoles, which can be switched by

the external field. The switching is hysteretic and fully reversible. Similar arguments have been reported in Ref. 26. In their paper, the field leads to the disintegration of the wall and the emission of skyrmions into the bulk. In this paper, we consider walls which are topologically protected and ferroelastic. The field can not destroy these walls but only tilt the induced dipoles inside the wall. As the walls remain uniform planes, no emission of skyrmion is expected but only rotational vortex structures.

We start the modeling from a simple toy model^{27,28} with dipolar interactions of two sub-lattices embedded into the ferroelastic model. The model was introduced in Ref. 29 for molecular dynamics (MDs) techniques to explore polar effects in complex ferroelastic domain patterns with many particles (e.g., 10^6 atoms) and long MD running times (e.g., 10^4 phonon times). We refer the reader to this paper for the details of the simulation. The model is based on simple non-linear elastic interactions (Landau springs) and harmonically coupled displacements of charged particles. The model is constructed such that the equilibrium single crystal (embedded in a 3-dimensional matrix) undergoes a tetragonal $4/mmm$ to orthorhombic mmm phase transition. Both phases are centrosymmetric. The symmetry is broken inside twin walls to non-centrosymmetric m , while additional symmetry breaking to 1 is possible by vortex structures.^{24,25} The bulk is hence ferroelastic, while the domain boundaries are polar. We then modify the bulk interactions with the same ferroelastic interaction but allow small dipoles in the bulk and observe how bulk dipoles interact with wall dipoles. The model parameters are inspired by SrTiO_3 with the energy scale determined by $T_c = 100$ K, a typical ferroelastic shear angle of 4° , and wall dipoles related to displacements of 6 pm as observed in CaTiO_3 .⁸

The initial configuration is a two-dimensional sandwich with two pre-existing horizontal domain boundaries (Fig. 1). The system size is $100a \times 102a$, where a ($= 0.1$ nm) is the lattice spacing. Periodic boundary conditions are adopted to

^{a)}E-mail: ekhard@esc.cam.ac.uk

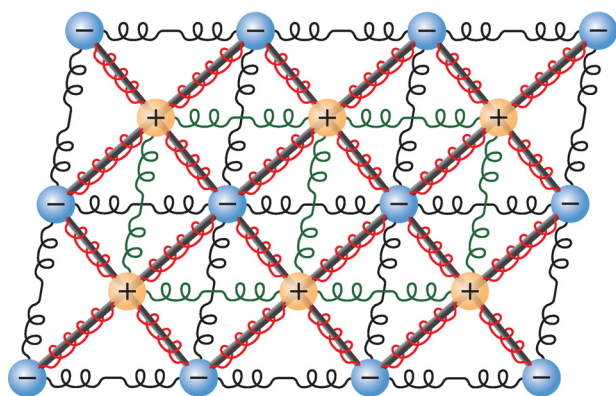


FIG. 1. Spring model with two charged sub-lattices. Coulomb interactions and interatomic interactions are combined in the model. The interatomic interactions between the nearest-neighbors are harmonic (shown by springs). Non-convex interactions (gray sticks) along diagonals in the ferroelastic sub-lattice lead to the formation of twin structures. The electrostatic interaction between the two sub-lattices combines with weak 2nd or 6th order springs are used to mimic the repulsive coupling between the sub-lattices. The spring stiffness for 2nd and 6th order potentials is 0.1 and 600, respectively.

avoid surface effects. We first studied the dipole configurations at different temperatures ranging from 0.1 K to 120 K, when the bulk ground state is paraelectric. The system was first relaxed using a conjugate gradient method to find the optimal position for each lattice point. Each configuration was then annealed at a given temperature for 5×10^5 time

steps. Next, we studied the dipole switching in response to the external electrical field. Here, the bulk ground state was chosen to be weakly polar so that the effect of the domain boundary on the enhanced polarity and the switching process became obvious. We applied the field along the direction perpendicular to the domain walls and increased the field linearly by steps of 0.5 mV/nm at 20 K. For each increment, the system is relaxed for 10^6 time steps. The configurations in the last 5×10^5 time steps were used to take time average. All the simulations were performed using the LAMMPS code.³⁰ NPT ensemble was used in the isothermal and isobaric simulations. The temperature of the sample was held constant by the Nosé-Hoover thermostat.^{31,32}

The macroscopic spontaneous strain is determined by the macroscopic shear angle of the bulk after annealing. It decreases with increasing temperature and shows a ferroelastic phase transition at $T_{\text{trans}} = 100$ K. The ferroelastic twin walls remain exactly at their initial positions (Figure 2(a)) after annealing at low temperatures. The atoms of the second sub-lattice are located at the inversion centers of the ferroelastic lattice so that no polarity is generated in the bulk (Figure 2(a)), in case of the non-polar bulk. Polarity was found inside the twin walls because the second sub-lattice shifts along the twin wall and breaks the inversion symmetry.¹⁹ The polar layers are two unit cells wide, similar to the experimental observations in CaTiO_3 (Refs. 8 and 12), which are insetted in Figure 2(a).

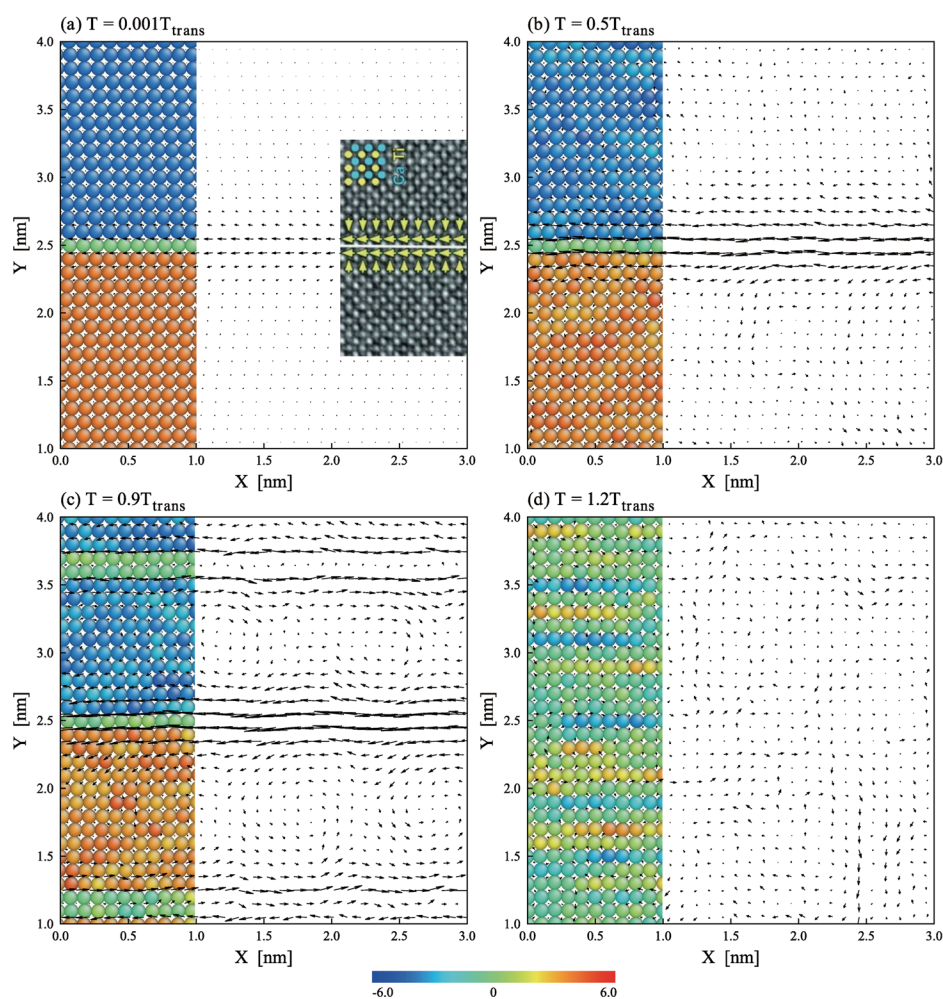


FIG. 2. Local dipole configuration and corresponding twin structure at four temperatures. Twin structure is visualized by ferroelastic sub-lattice, while the second sub-lattice is omitted for clarity. The color scheme represents the vertical local shear angle in units of degrees. (a) Time averaged dipole configuration shows polarity around the twin walls but not in the bulk. A polar twin wall in CaTiO_3 is shown in the inset.⁸ Thermal excitation leads to the disorder and vortices (b) and (c). (d) Polarity disappears in paraelectric phase where no twin boundaries exit. Note that dipole displacements are amplified by a factor of 40.

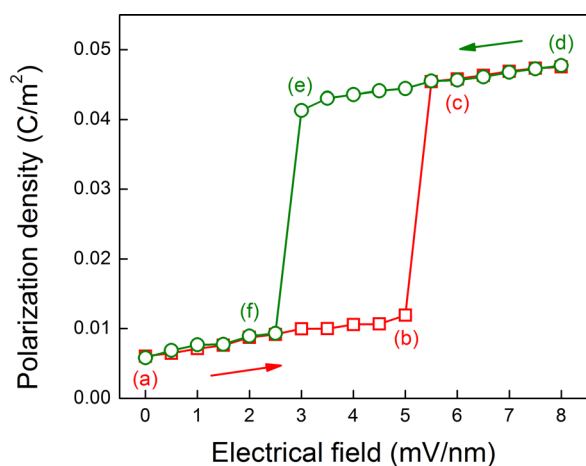


FIG. 3. Ferroelectric hysteresis for competing bulk and wall dipoles.

Increasing temperature leads to structural disorder both in the bulk and at the twin boundaries (Figures 2(b) and 2(c)). The overall effect remains the same as at low temperatures: No polarity was found after thermal averaging inside the bulk, while all twin boundaries are polar. Additional twin boundaries nucleate at high temperatures slightly below T_{trans} . At these temperatures, we find high twin wall densities and large dipole moments in the bulk near the twin boundaries. These dipoles form vortices whereby one edge of each vortex is constituted by the dipoles in the twin wall (Figure 2(c)). The diameters of the vortices are some 5 unit cells, as shown in Figure 2(c). If the twin walls are sufficiently close to each other, vortices fluctuate with short lifetimes. A similar vortex effect was previously reported in SrTiO_3 .^{14,15} Near the transition point, we observe the expected divergency of the thickness of the twin wall that is well known from the continuums description within Landau theory.¹³

We now allow weak bulk polarity with a double well potential with a weak repulsive 6th order term and attractive

Coulomb interactions for the anion-cation interaction. Decreasing the bulk polarity to zero would then define incipient ferroelectricity as in SrTiO_3 and KTaO_3 . Starting from a field-free condition, we ramp up the electrical field along y direction (perpendicular to twin walls). The maximum value of external field is 8 mV/nm. To study the ferroelectric hysteresis, the field is decreased from the maximum value back to zero linearly. Figure 3 shows the variation of polarization density with external electrical field. Here, the polarization density is defined as qs/V , where q is the electron charge, s is the averaged polarization displacement, and V is the system volume. We find that the polarization density increases gradually with the applying of field when the field is weak. The polarization undergoes a large jump when the field reaches 6 mV/nm. After the jump, the system possesses the permanent polarization. It forms a complete hysteresis loop when we decreased the field to zero.

Figure 4 shows the corresponding dipole configurations marked in Fig. 3. We find two competing displacements. The field induces vertical dipoles in the bulk and rotates the wall dipoles. The geometrical effect is that rotations of the dipoles near the twin boundaries lead to vortex-like structures. As adjacent twin boundaries will always generate dipoles in opposite directions, the induced bulk polarity has hence to rotate between the two walls. We find that this rotation occurs over fewer than ten lattice distances and is hence very localized. Furthermore, the rotation does not occur in the middle between the two walls but is attached to one wall. These rotations are like wide 180° ferroelectric walls attached to a ferroelastic wall. The rotating walls distort the ferroelastic lattice, which appears to add to the rapprochement of the vortex layer to the twin wall. The increasing external field destroys the vortex at the coercive field, and all dipoles rotate towards the field direction. The fundamental reason for the ferroelectric hysteresis in Fig. 3 is hence the appearance of the vortex for small fields and its destruction

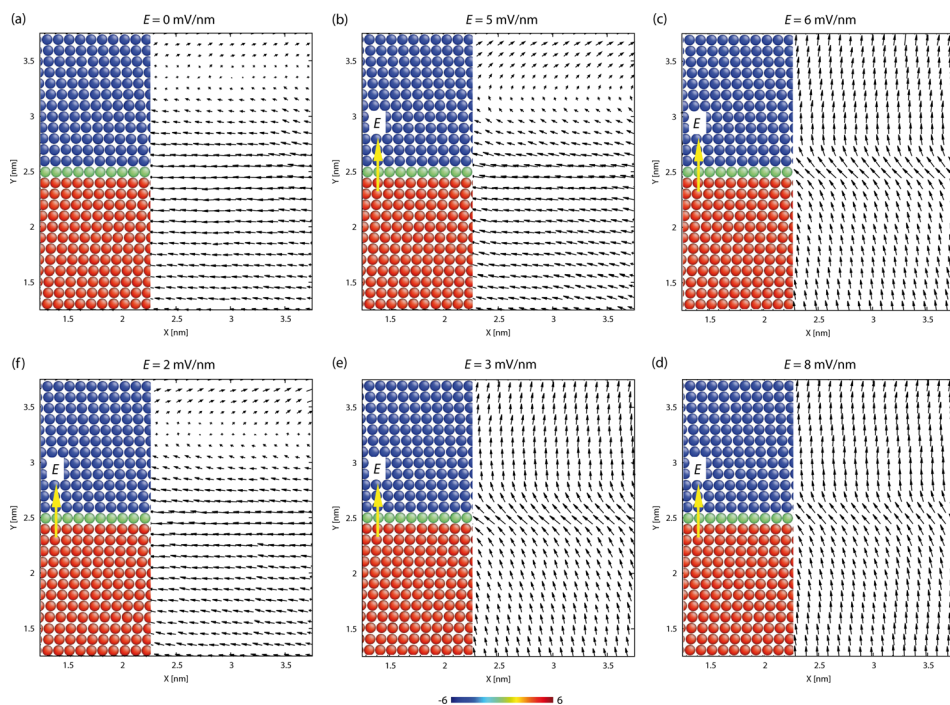


FIG. 4. Strain and dipole pattern with interactions between the strongly polar twin walls and a weakly polar bulk. The field is applied in the vertical direction (yellow arrow), which is perpendicular to the twin boundary. The dipoles in the wall are rotated by the field at 90° . Vortex states between the horizontal dipoles in the twin walls and the inclined dipoles in the bulk are seen for small fields. Large fields destroy the vortex and lead to an overall vertical orientation of the dipoles, while the horizontal components for the wall dipoles are visible even for the largest fields. Dipole displacements are amplified by a factor of 20.

for fields larger than the coercive field. The sample polarization in Fig. 3 is the total sample polarization (wall and bulk) and will scale with the respect to the domain size. Similarly, the coercive field will scale with the wall density. This effect can become important when new domain walls nucleate when heating towards the ferroelastic transition point, while thermal effects will lower the coercive field. Further work to investigate the scaling properties is under way.

E.K.H.S. was grateful to EPSRC (EP/K009702/1) for support. S.L. and P.G. appreciate the support by Alexander von Humboldt Foundation. Z.Z. and X.D. are grateful to NSFC (Nos. 51171140, 51321003, and 51320105014) for financial support. Z.Z. was supported by a scholarship from the China Scholarship Council.

¹H. Ishii, K. Sugiyama, E. Ito, and K. Seki, *Adv. Mater.* **11**, 605 (1999).

²J. Mannhart and D. G. Schlom, *Science* **327**, 1607 (2010).

³P. Zubko, S. Gariglio, M. Gabay, P. Ghosez, and J. M. Triscone, *Annu. Rev. Condens. Matter Phys.* **2**, 141 (2011).

⁴D. Wang, E. K. H. Salje, S.-B. Mi, C. L. Jia, and L. Bellaiche, *Phys. Rev. B* **88**, 134107 (2013).

⁵A. Aird and E. K. H. Salje, *J. Phys.: Condens. Matter* **10**, L377 (1998).

⁶L. Goncalves-Ferreira, S. A. T. Redfern, E. Artacho, E. Salje, and W. T. Lee, *Phys. Rev. B* **81**, 024109 (2010).

⁷L. Goncalves-Ferreira, S. A. T. Redfern, E. Artacho, and E. K. H. Salje, *Phys. Rev. Lett.* **101**, 097602 (2008).

⁸S. Van Aert, S. Turner, R. Delville, D. Schryvers, G. Van Tendeloo, and E. K. H. Salje, *Adv. Mater.* **24**, 523 (2012).

⁹H. Yokota, H. Usami, R. Haumont, P. Hicher, J. Kaneshiro, E. K. H. Salje, and Y. Uesu, *Phys. Rev. B* **89**, 144109 (2014).

¹⁰K. L. Kobayashi, T. Kimura, H. Sawada, K. Terakura, and Y. Tokura, *Nature* **395**, 677 (1998).

¹¹E. Salje and H. Zhang, *Phase Transitions* **82**, 452 (2009).

¹²E. K. H. Salje, *ChemPhysChem* **11**, 940 (2010).

¹³E. K. H. Salje, *Annu. Rev. Mater. Res.* **42**, 265 (2012).

¹⁴J. Seidel, L. W. Martin, Q. He, Q. Zhan, Y. H. Chu, A. Rother, M. E. Hawkrige, P. Maksymovych, P. Yu, M. Gajek *et al.*, *Nat. Mater.* **8**, 229 (2009).

¹⁵G. Catalan, J. Seidel, R. Ramesh, and J. F. Scott, *Rev. Mod. Phys.* **84**, 119 (2012).

¹⁶J. Seidel, P. Maksymovych, Y. Batra, A. Katan, S. Y. Yang, Q. He, A. P. Baddorf, S. V. Kalinin, C. H. Yang, J. C. Yang, *et al.*, *Phys. Rev. Lett.* **105**, 197603 (2010).

¹⁷N. Leo, A. Bergman, A. Cano, N. Poudel, B. Lorenz, M. Fiebig, and D. Meier, *Nat. Commun.* **6**, 6661 (2015).

¹⁸D. Meier, J. Seidel, A. Cano, K. Delaney, Y. Kumagai, M. Mostovoy, N. A. Spaldin, R. Ramesh, and M. Fiebig, *Nat. Mater.* **11**, 284 (2012).

¹⁹C. J. M. Daumont, S. Farokhipoor, A. Ferri, J. C. Wojdel, B. J. Kooi, and B. Noheda, *Phys. Rev. B* **81**, 144115 (2010).

²⁰S. Farokhipoor and B. Noheda, *Phys. Rev. Lett.* **107**, 127601 (2011).

²¹A. K. Tagantsev, E. Courtens, and L. Arzel, *Phys. Rev. B* **64**, 224107 (2001).

²²P. Zubko, G. Catalan, and A. K. Tagantsev, *Annu. Rev. Mater. Res.* **43**, 387 (2013).

²³E. K. H. Salje and J. F. Scott, *Appl. Phys. Lett.* **105**, 252904 (2014).

²⁴T. Zykova-Timan and E. K. H. Salje, *Appl. Phys. Lett.* **104**, 082907 (2014).

²⁵B. Houchmandzadeh, J. Lajzerowicz, and E. Salje, *J. Phys.: Condens. Matter* **3**, 5163 (1991).

²⁶M. Dawber, A. Gruverman, and J. F. Scott, *J. Phys.: Condens. Matter* **18**, L71 (2006).

²⁷E. K. H. Salje, X. Ding, Z. Zhao, T. Lookman, and A. Saxena, *Phys. Rev. B* **83**, 104109 (2011).

²⁸Z. Zhao, X. Ding, J. Sun, and E. K. H. Salje, *J. Phys.: Condens. Matter* **26**, 142201 (2014).

²⁹Z. Zhao, X. Ding, and E. K. H. Salje, *Appl. Phys. Lett.* **105**, 112906 (2014).

³⁰S. Plimpton, *J. Comput. Phys.* **117**, 1 (1995).

³¹S. Nose, *J. Chem. Phys.* **81**, 511 (1984).

³²W. G. Hoover, *Phys. Rev. A* **31**, 1695 (1985).